

Neutron in Strong Magnetic Fields

M.A. Andreichikov, B.O. Kerbikov,
Moscow Institute of Physics and Technology,
Dolgoprudny, Institutskiy Pereulok 9, 141700 Moscow Region, Russia,
State Research Center
Institute of Theoretical and Experimental Physics,
Moscow, 117218 Russia

V.D. Orlovsky, Yu.A. Simonov
State Research Center
Institute of Theoretical and Experimental Physics,
Moscow, 117218 Russia

September 3, 2018

Abstract

Relativistic world-line Hamiltonian for strongly interacting $3q$ systems in magnetic field is derived from the path integral for the corresponding Green's function. The neutral baryon Hamiltonian in magnetic field obeys the pseudomomentum conservation and allows a factorization of the c.m. and internal motion. The resulting expression for the baryon mass in magnetic field is written explicitly with the account of hyperfine, OPE and OGE (color Coulomb) interaction. The neutron mass is fast decreasing with magnetic field, losing 1/2 of its value at $eB \sim 0.25 \text{ GeV}^2$ and is nearly zero at $eB \sim 0.5 \text{ GeV}^2$. Possible physical consequences of the calculated mass trajectory of the neutron, $M_n(B)$, are presented and discussed.

1 Introduction

The properties of strongly interacting matter under extreme conditions are challenging to study both from experimental and theoretical sides. Currently a great interest attracts the response of baryon and quark matter to intense magnetic field (MF) [1]. The outbreak of interest to this subject is caused by the fact that MF of the order of $eB \sim \Lambda_{QCD}^2 \sim 10^{19} \text{G}$ ($\text{GeV}^2 \simeq 5.12 \cdot 10^{19} \text{G}$) became a physical reality. Such MF is created (for a short time) in peripheral heavy ion collisions at RHIC and LHC [2]. The field about four orders of magnitude less exists on the surface of magnetars and it may be of the order of 10^{17}G in its interior [3]. MF, as high as $(100 \text{ MeV})^2$, can change the internal structure of baryons and affect the possible neutron matter \rightarrow quark matter transition, since MF can influence the phase structure of the QCD vacuum [4]. Prior to analyzing the behavior of bulk neutron matter embedded in MF one should understand what happens to a neutron in MF. What are the changes that occur to its mass, shape and decay properties? Similar questions were raised before in regard to the hydrogen atom and positronium [5]. In case of the hydrogen atom it was shown that in superstrong MF radiative corrections screen the Coulomb potential thus preventing the “fall to the center” phenomenon. As for the positronium, the collapse was predicted at super-high MF $eB \gtrsim 10^{40} \text{G}$ [6].

The situation with hadron masses in presence of strong MF demands an analysis at the quark level based on the fundamental QCD principles. Quark structure comes into play when the Landau radius $r_H = (eB)^{-1/2}$ becomes equal or smaller than the size of the hadron. For example, the value of MF which corresponds to $r_H = 0.6 \text{ fm}$ is $eB \simeq 5 \cdot 10^{18} \text{ G}$. The first results obtained at the quark level have been acquired in two different approaches: on the lattice [7, 8], and analytically [9, 10, 11, 12, 13]. Analytical results [9, 10, 11, 12] were obtained using the QCD path integral technique and the relativistic world-line Hamiltonian [14, 15]. Our results presented in [10] are in agreement with the lattice data [7, 8], in the region $eB \leq 5 \text{ GeV}^2$, where lattice calculations in MF are reliable.

Performing the analytic calculations of meson spectra without quark loop corrections in gluon exchange in [9] we observed that meson mass tends to zero due to enhanced color Coulomb interaction. This phenomenon, which may be called “The magnetic collapse in QCD”, occurs in the large N_c limit, when the contribution of quark loops is negligible. Below we show that the same situation is encountered in the neutron, again in absence of quark loops.

However, the inclusion of quark loop effects, done in [11], eliminates the problem of “magnetic collapse” in meson, and as we show below, the same is true for baryons. Instead, one encounters in mesons the problem of the strong enhancement of the wave function at small distances, which in turn leads to the amplification of the hyperfine(hf) interaction – the “magnetic focusing” effect, first found in hydrogen [16] and in any system in MF, which contain oppositely charged components [17]. This makes the π^0 mass at large eB rather small, as it was found on the lattice [7] and in the Nambu-Goldstone type of analysis in [12]. We show below that the neutron mass also becomes small in strong MF due to color Coulomb and hf interactions. Moreover, the first order hf contribution produce, zero neutron mass at some B_{crit} , and even the smearing of the hf term, which makes meson masses nonvanishing [10], does not prevent the vanishing of the neutron mass. However, the theorem of [18] forbids the vanishing of the mass due to MF, which implies that higher orders make this mass finite, however small.

The main result of the paper is the fast decrease of the neutron mass, what poses some questions to the dynamics of the neutron stars in strong MF and their possible transitions into quark stars.

To evaluate the baryon spectra one has to overcome several difficulties. The first problem is to develop the relativistic formalism for three particles with nonperturbative interaction. The formalism of this kind is the 3-body world-line Hamiltonian [19, 20], obtained for zero MF from the Fock-Feynman-Schwinger path integral [14] and used in [18, 21, 22] for baryon spectrum. We consider this formalism in the case of three quarks in Section 2. We also show there, that in the neutral $3q$ system one can introduce pseudomomentum and exactly factorize the center of mass (c.m.) and relative motion, as it was done in the neutral 2-body system [23]. In this way the classical factorization problem in MF, studied for decades for the neutral 2-body system, is solved here for the neutral 3-body system with arbitrary masses and charges both in nonrelativistic and relativistic context. In Section 3 we treat confinement, using for it a simplified quadratic form, which allows to find the wave function analytically with 5% accuracy for eigenvalues, and write down the spin-flavor part of the wave function. In Section 4 we estimate the contribution of OGE (color Coulomb) interaction $\langle V_{\text{Coul}} \rangle$ for three quarks with obtained wave functions, first using gluon loop (asymptotic freedom) form, and then quark loop contribution. In Section 5 we study the spin structure of the wave function and spin splitting in MF. The situation here is similar to the spectrum of hydrogen atom or meson with hyperfine

and magnetic moment interaction included. The subtle point is that the use of hf interaction proportional to the δ -function at the origin in the first order perturbation theory, which results in vanishing of the neutron mass at large MF. In addition to the observed spin splitting in baryons is much stronger than in mesons, and one must introduce additional sources of the spin-spin interaction, the OPE forces, which are also subject to MF. In Section 6 all pieces of the baryon mass are collected and results of numerical calculations for the total mass are presented as a function of MF. Section 7 is devoted to the discussion of the results and their physical significance. Concluding remarks are in Section 8 together with future prospects. Three Appendices contain the details of the calculations.

2 Baryons in magnetic field

Our approach to the problem of neutron properties in MF is based on recently developed theory of quark-antiquark system in MF [10]. The starting point is the Feynman-Schwinger (world-line) representation of the quark Green's function. The same formalism for baryons in absence of MF was developed in [19, 20, 22] and successfully used in [24]. Here we accommodate the treatment of MF from [10] to the three-body relativistic Hamiltonian of [19, 20, 22]. Consider a neutron as a three-quark system with d -quarks at positions $\mathbf{z}^{(1)}$ and $\mathbf{z}^{(2)}$, and u -quark at $\mathbf{z}^{(3)}$. The relativistic free motion Hamiltonian has the form

$$H_0 = \frac{1}{2\omega_+} \mathbf{P}^2 + \frac{1}{2\omega} \boldsymbol{\pi}^2 + \frac{1}{2\omega} \mathbf{q}^2 + \sum_{i=1}^3 \frac{m_i^2 + \omega_i^2}{2\omega_i}. \quad (1)$$

Here the momenta \mathbf{P} , $\boldsymbol{\pi}$ and \mathbf{q} correspond to the Jacobi coordinates

$$\mathbf{P} = -i \frac{\partial}{\partial \mathbf{R}}, \quad \boldsymbol{\pi} = -i \frac{\partial}{\partial \boldsymbol{\eta}}, \quad \mathbf{q} = -i \frac{\partial}{\partial \boldsymbol{\xi}}, \quad (2)$$

where

$$\begin{cases} \mathbf{R} = \frac{1}{\omega_+} \sum \omega_i \mathbf{z}^{(i)}, \\ \boldsymbol{\eta} = \frac{\mathbf{z}^{(2)} - \mathbf{z}^{(1)}}{\sqrt{2}}, \\ \boldsymbol{\xi} = \sqrt{\frac{\omega_3}{2\omega_+}} (\mathbf{z}^{(1)} + \mathbf{z}^{(2)} - 2\mathbf{z}^{(3)}). \end{cases} \quad (3)$$

The i -th quark current mass is m_i , the quantities ω_i play the role of constituent masses, we denote $\omega_1 = \omega_2 \equiv \omega$, $\omega_u = \omega_3$, $\omega_+ = 2\omega + \omega_3$. The

momenta \mathbf{P} , $\boldsymbol{\pi}$ and \mathbf{q} are related to the momenta of individual quarks by

$$p_k^{(i)} = \alpha_i P_k + \beta_i q_k + \gamma_i \pi_k, \quad (4)$$

$$p_k^{(1)} = \frac{\omega}{\omega_+} P_k + \sqrt{\frac{\omega_3}{2\omega_+}} q_k - \frac{1}{\sqrt{2}} \pi_k, \quad (5)$$

$$p_k^{(2)} = \frac{\omega}{\omega_+} P_k + \sqrt{\frac{\omega_3}{2\omega_+}} q_k + \frac{1}{\sqrt{2}} \pi_k, \quad (6)$$

$$p_k^{(3)} = \frac{\omega_3}{\omega_+} P_k - \sqrt{\frac{2\omega_3}{\omega_+}} q_k. \quad (7)$$

In (1) the center-of-mass motion decouples and can be removed from the Hamiltonian.

For a neutral three-body and in general for a neutral N -body nonrelativistic system embedded in MF factorization of the center-of-mass motion is possible using the conserved pseudomomentum [23, 26]. The realization of the factorization procedure depends on the relation between the masses and charges of the three particles forming the system. For the neutron $m_1 = m_2 = m_d$, $m_3 = m_u$, $e_1 = e_2 = -e/2$, $e_3 = e$. In strong MF we shall consider for simplicity the case of symmetrical spin configuration, when both d -quarks have the same spin orientation, opposite to that of u -quark. As will be seen, these states provide the highest and the lowest energy eigenvalues at large B . For such a configuration the problem was solved in [25] both in the nonrelativistic and relativistic case. Below we follow the results obtained there. With MF included the Hamiltonian has the form

$$H_0 = \sum_{i=1}^3 \frac{(p_k^{(i)} - e_i A_k)^2 + m_i^2 + \omega_i^2}{2\omega_i}, \quad (8)$$

choosing the gauge $\mathbf{A} = \frac{1}{2}(\mathbf{B} \times \mathbf{z})$ and passing to the Jacobi coordinates (3)

and momenta (2) we have

$$\begin{aligned}
H_0 = & \frac{1}{2\omega} \left[\frac{\omega}{\omega_+} \mathbf{P} + \sqrt{\frac{\omega_3}{2\omega_+}} \mathbf{q} - \frac{\pi}{\sqrt{2}} + \frac{e}{4} \left(\mathbf{B} \times \left(\mathbf{R} + \sqrt{\frac{\omega_3}{2\omega_+}} \boldsymbol{\xi} - \frac{\boldsymbol{\eta}}{\sqrt{2}} \right) \right) \right]^2 + \\
& + \frac{1}{2\omega} \left[\frac{\omega}{\omega_+} \mathbf{P} + \sqrt{\frac{\omega_3}{2\omega_+}} \mathbf{q} + \frac{\pi}{\sqrt{2}} + \frac{e}{4} \left(\mathbf{B} \times \left(\mathbf{R} + \sqrt{\frac{\omega_3}{2\omega_+}} \boldsymbol{\xi} + \frac{\boldsymbol{\eta}}{\sqrt{2}} \right) \right) \right]^2 + \\
& + \frac{1}{2\omega_3} \left[\frac{\omega_3}{\omega_+} \mathbf{P} - \sqrt{\frac{2\omega_3}{\omega_+}} \mathbf{q} - \frac{e}{2} \left(\mathbf{B} \times \left(\mathbf{R} - \sqrt{\frac{2\omega^2}{\omega_+\omega_3}} \boldsymbol{\xi} \right) \right) \right]^2 + \\
& + \sum_{i=1}^3 \frac{m_i^2 + \omega_i^2}{2\omega_i} \equiv \frac{1}{2\omega} \left((\mathbf{J}^{(1)})^2 + (\mathbf{J}^{(2)})^2 \right) + \frac{1}{2\omega_3} (\mathbf{J}^{(3)})^2 + \sum_{i=1}^3 \frac{m_i^2 + \omega_i^2}{2\omega_i}. \quad (9)
\end{aligned}$$

The conserved pseudo-momentum for this system reads

$$\hat{\mathbf{F}} = \mathbf{P} - \frac{e}{2} \sqrt{\frac{\omega_+}{2\omega_3}} (\mathbf{B} \times \boldsymbol{\xi}). \quad (10)$$

The neutron wave function in MF is an eigenfunction of $\hat{\mathbf{F}}$ with the eigenvalue \mathbf{F}

$$\hat{\mathbf{F}} \Psi(\mathbf{R}, \boldsymbol{\xi}, \boldsymbol{\eta}) = \mathbf{F} \Psi(\mathbf{R}, \boldsymbol{\xi}, \boldsymbol{\eta}). \quad (11)$$

The existence of the conserved pseudo-momentum allows to represent the wave function in the form $\Psi(\mathbf{R}, \boldsymbol{\xi}, \boldsymbol{\eta}) = e^{i\boldsymbol{\nu}\mathbf{R}} \varphi(\boldsymbol{\xi}, \boldsymbol{\eta})$ and to find the phase $\boldsymbol{\nu}$ from the eigenvalue equation (11). We obtain

$$\Psi(\mathbf{R}, \boldsymbol{\xi}, \boldsymbol{\eta}) = \exp \left\{ i \left[\mathbf{F} + \frac{e}{2} \sqrt{\frac{\omega_+}{2\omega_3}} (\mathbf{B} \times \boldsymbol{\xi}) \right] \mathbf{R} \right\} \varphi(\boldsymbol{\xi}, \boldsymbol{\eta}). \quad (12)$$

Applying $J_k^{(i)} \Psi$ to the wave function (12) one gets

$$(\mathbf{J}^{(1)})^2 e^{i\boldsymbol{\nu}\mathbf{R}} \varphi = e^{i\boldsymbol{\nu}\mathbf{R}} \left[\sqrt{\frac{\omega_3}{2\omega_+}} \left(-i \frac{\partial}{\partial \boldsymbol{\xi}} \right) + \mathbf{C}^{(1)} \right]^2 \varphi, \quad (13)$$

$$(\mathbf{J}^{(2)})^2 e^{i\boldsymbol{\nu}\mathbf{R}} \varphi = e^{i\boldsymbol{\nu}\mathbf{R}} \left[\sqrt{\frac{\omega_3}{2\omega_+}} \left(-i \frac{\partial}{\partial \boldsymbol{\xi}} \right) + \mathbf{C}^{(2)} \right]^2 \varphi, \quad (14)$$

$$(\mathbf{J}^{(3)})^2 e^{i\boldsymbol{\nu}\mathbf{R}} \varphi = e^{i\boldsymbol{\nu}\mathbf{R}} \left[\sqrt{\frac{2\omega_3}{\omega_+}} \left(-i \frac{\partial}{\partial \boldsymbol{\xi}} \right) - \mathbf{C}^{(3)} \right]^2 \varphi, \quad (15)$$

where

$$\mathbf{C}^{(1)} = \frac{\omega}{\omega_+} \mathbf{F} + \frac{e}{4} \sqrt{\frac{\omega_+}{2\omega_3}} (\mathbf{B} \times \boldsymbol{\xi}) - \frac{\boldsymbol{\pi}}{\sqrt{2}} - \frac{e}{4\sqrt{2}} (\mathbf{B} \times \boldsymbol{\eta}), \quad (16)$$

$$\mathbf{C}^{(2)} = \mathbf{C}^{(1)} (\boldsymbol{\pi} \rightarrow -\boldsymbol{\pi}, \boldsymbol{\eta} \rightarrow -\boldsymbol{\eta}), \quad (17)$$

$$\mathbf{C}^{(3)} = \frac{\omega_3}{\omega_+} \mathbf{F} + \frac{e}{4} \sqrt{\frac{2\omega_+}{\omega_3}} (\mathbf{B} \times \boldsymbol{\xi}). \quad (18)$$

In (13)-(15) the following combinations appear:

$$(\mathbf{B} \times \boldsymbol{\xi})_k \frac{\partial \varphi}{i \partial \xi_k} = B_k L_k^{(\xi)} \varphi, \quad L_k^{(\xi)} = e_{klm} \xi_l \frac{\partial}{i \partial \xi_m}, \quad (19)$$

$$(\mathbf{B} \times \boldsymbol{\eta})_k \frac{\partial \varphi}{i \partial \eta_k} = B_k L_k^{(\eta)} \varphi, \quad L_k^{(\eta)} = e_{klm} \eta_l \frac{\partial}{i \partial \eta_m}. \quad (20)$$

Note that the two orbital momenta $\mathbf{L}^{(\xi)}$ and $\mathbf{L}^{(\eta)}$ are independent and commute with each other. Finally from (9) one obtains for $\mathbf{F} = 0$,

$$\begin{aligned} H_0 = & -\frac{1}{2\omega} (\Delta_\xi + \Delta_\eta) + \frac{1}{2\omega} \left(\frac{eB}{4} \right)^2 \left(\frac{\omega_+^2}{\omega_3^2} \boldsymbol{\xi}_\perp^2 + \boldsymbol{\eta}_\perp^2 \right) + \\ & + \frac{e\mathbf{B}}{4\omega} \left(\frac{\omega_3 - 2\omega}{\omega_3} \mathbf{L}^{(\xi)} + \mathbf{L}^{(\eta)} \right) + \sum_{i=1}^3 \frac{m_i^2 + \omega_i^2}{2\omega_i}. \end{aligned} \quad (21)$$

A word of caution is in order here. One can safely put $\mathbf{F} = 0$ at the ground state only when the interparticle potential is a harmonic oscillator one [23, 26, 13], otherwise the ground state may require nonzero \mathbf{F} , as it happens in the nonrelativistic treatment of heavy quarkonia [13]. Below we show that with the high accuracy confinement may be represented in a such form.

Next we add the interaction terms to the Hamiltonian following the approach developed in [10] for mesons. The complete Hamiltonian has the form

$$H^{(B)} = H_0 + V_\sigma + V_{\text{conf}} + V_{\text{Coul}} + \Delta_{SE} + \Delta_{\text{string}} + \Delta_{SD}. \quad (22)$$

Here

$$V_\sigma = - \sum_{i=1}^3 \frac{e_i \boldsymbol{\sigma}^{(i)} \mathbf{B}}{2\omega_i}, \quad V_{\text{conf}} = \sigma \sum_{i=1}^3 |\mathbf{z}^{(i)} - \mathbf{z}_Y|, \quad (23)$$

where \mathbf{z}_Y is the string junction position (Torricelli point),

$$V_{\text{Coul}} = -\frac{2}{3} \sum_{i>j} \frac{\alpha_s(r_{ij})}{r_{ij}}, \quad r_{ij} \equiv |\mathbf{z}^{(i)} - \mathbf{z}^{(j)}|, \quad (24)$$

$$\Delta_{SE} = -\frac{3\sigma}{4\pi} \sum_{i=1}^3 \frac{1 + \eta(\lambda(\sqrt{2eB + m_i^2}))}{\omega_i}, \quad (25)$$

where $\eta(t) = t \int_0^\infty z^2 K_1(tz) e^{-z} dz$ and $\lambda \sim 1 \text{ GeV}^{-1}$ is vacuum correlation lengths,

$$\Delta V_{\text{string}} = - \sum \frac{l_i^2 \sigma \langle r_i^{-1} \rangle}{2 \langle \sigma r_i \rangle (\omega_i + \frac{1}{3} \langle \sigma r_i \rangle)}, \quad r_i = |\mathbf{z}_i - \mathbf{z}_Y|, \quad (26)$$

Δ_{SE} is quark self-energy [27], l_i is the angular momentum of the quark i . The spin-dependent interaction can be splitted into four terms,

$$\Delta_{SD} = \Delta_{ss}^{\text{pert}} + \Delta_{ss}^{\text{nonp}} + \Delta_{SO}^{\text{pert}} + \Delta_{SO}^{\text{nonp}}, \quad (27)$$

and, e.g.,

$$\Delta_{ss}^{\text{pert}} = \sum_{i<j} \frac{\boldsymbol{\sigma}^{(i)} \boldsymbol{\sigma}^{(j)} V_4(r_{ij}) + [3(\boldsymbol{\sigma}^{(i)} \mathbf{n})(\boldsymbol{\sigma}^{(j)} \mathbf{n}) - \boldsymbol{\sigma}^{(i)} \boldsymbol{\sigma}^{(j)}] V_3(r_{ij})}{24\omega_i \omega_j} \quad (28)$$

with

$$V_4(r) = \frac{32\pi\alpha_s}{3} \delta^{(3)}(\mathbf{r}), \quad V_3(r) = \frac{4\alpha_s}{r^3}. \quad (29)$$

In what follows the tensor contribution proportional to V_3 in (28) will be neglected. The reason is twofold. First, we shall be interested in lowest states with $l_i = 0$. However, even in this case tensor forces may be present due to deformation of the wave function in MF, as it happens with the hydrogen atom [16]. Below it will be shown that this can occur only at $eB \gg \sigma \simeq 10^{19} \text{ G}$. Therefore the second reason to ignore V_3 is that this term is irrelevant at $eB \lesssim 10^{19} \text{ G}$. The term $\Delta_{ss}^{\text{nonp}}$ appears to be much smaller than $\Delta_{ss}^{\text{pert}}$ and will be neglected. For more details on spin-dependent terms in absence of MF see [20], and for the case of nonzero MF a detailed derivation is given in [18], where it is shown that the MF induced tensor forces are tending to zero at very large MF. There also the terms $\Delta_{ss}^{\text{pert}}$, $\Delta_{ss}^{\text{nonp}}$ and Δ_{SE} are derived explicitly.

3 Simplification for lowest levels

As in the case of mesons, we shall replace V_{conf} by the quadratic expression, which after minimization with respect to parameter γ approaches the original form (3).

$$\begin{aligned} V_{\text{conf}} = \sigma \sum_{i=1}^3 |\mathbf{z}^{(i)} - \mathbf{z}_Y| &\rightarrow V_{\text{conf}}^{(\gamma)} = \frac{\sigma}{2} \left\{ \sum_{i=1}^3 \left[\frac{(\mathbf{z}^{(i)} - \mathbf{z}_Y)^2}{\gamma} \right] + 3\gamma \right\} = \\ &= 3\frac{\sigma\gamma}{2} + \frac{\sigma}{2\gamma} \sum_{i=1}^3 (\mathbf{z}^{(i)} - \mathbf{z}_Y)^2. \end{aligned} \quad (30)$$

Minimization yields

$$\min_{\gamma} V_{\text{conf}}^{(\gamma)} = \sigma \left\{ \sum_{i=1}^3 (\mathbf{z}^{(i)} - \mathbf{z}_Y)^2 \right\}^{1/2} \leq \sigma \sum_{i=1}^3 \{ (\mathbf{z}^{(i)} - \mathbf{z}_Y)^2 \}^{1/2} = V_{\text{conf}}. \quad (31)$$

We approximate the Torricelli point \mathbf{z}_Y by the c.m. point. This is reasonable for equal or small masses. Passing to the Jacobi coordinates we get the final expression

$$V_{\text{conf}}^{(\gamma)} = \frac{3\sigma\gamma}{2} + \frac{\sigma}{2\gamma} \left(\frac{\omega_3^2 + 2\omega^2}{\omega_+ \omega_3} \boldsymbol{\xi}^2 + \boldsymbol{\eta}^2 \right). \quad (32)$$

As in the case of mesons, we take the average value $\langle V_{\text{Coul}} \rangle$ of the OGE operator (24) and of $\Delta_{ss}^{\text{pert}}$ with the wave function $\Psi(\boldsymbol{\xi}, \boldsymbol{\eta})$, corresponding to $H_0 + V_{\text{conf}}^{(\gamma)}$. The resulting energy eigenvalue can be considered as an upper limit for the actual energy eigenvalue. From (21) and (32) it is clear that this wave function factorizes, $\varphi(\boldsymbol{\xi}, \boldsymbol{\eta}) = \chi(\boldsymbol{\xi})\phi(\boldsymbol{\eta})$.

Similarly to what happens in the case of the $q\bar{q}$ system [10], for $eB \gg \sigma$ our system acquires the form of an elongated ellipsoid with large axis $r_0 \approx \frac{1}{\sqrt{\sigma}}$ and small axis $r_B = \frac{1}{\sqrt{eB}}$. This results in the increase of the Coloumb term $\langle V_{\text{Coul}} \rangle$ asymptotically as $\ln(\ln \frac{eB}{\sigma})$. As will be seen, the inclusion of quark loops in the gluon exchange stabilizes the energy of the 3-body system as in the case of mesons, discussed in [11].

Finally $\Delta_{ss}^{\text{pert}}$ is considered as a correction with the average value $\langle \Delta_{ss}^{\text{pert}} \rangle$ calculated with the wave functions which are the eigenfunctions of the equation

$$(H_0 + V_{\sigma} + V_{\text{conf}})\varphi(\boldsymbol{\eta}, \boldsymbol{\xi}) = M_0(\omega_i, \gamma)\varphi(\boldsymbol{\eta}, \boldsymbol{\xi}). \quad (33)$$

The final expression for the baryon mass is

$$M(B) = \bar{M}_0(B) + \Delta_{SE}(\omega_i^{(0)}) + \langle V_{\text{Coul}}(\omega_i^{(0)}) \rangle + \langle \Delta_{ss}^{\text{pert}}(\omega_i^{(0)}) \rangle, \quad (34)$$

where $\bar{M}_0(B)$ is obtained inserting into $M_0(\omega_i, \gamma)$ the extremal values of ω_i and γ , obtained from the conditions

$$\left. \frac{\partial M_0(\omega_i, \gamma)}{\partial \omega_i} \right|_{\omega_i = \omega_i^{(0)}} = 0, \quad \left. \frac{\partial M_0(\omega_i, \gamma)}{\partial \gamma} \right|_{\gamma = \gamma^{(0)}} = 0. \quad (35)$$

We remind, that the equation (33) admits a separable solution $\varphi(\boldsymbol{\eta}, \boldsymbol{\xi}) = \phi(\boldsymbol{\eta})\chi(\boldsymbol{\xi})$ with ϕ and χ being explicit oscillator functions yielding the exact answer for $M_0(\omega_i, \gamma_i)$.

The total baryon wave function can be written as

$$\begin{aligned} \Psi_B = & [\Psi^{\text{symm}}(\boldsymbol{\xi}, \boldsymbol{\eta})\psi^{\text{symm}}(\sigma, f) + \Psi'(\boldsymbol{\xi}, \boldsymbol{\eta})\psi'(\sigma, f) + \\ & + \Psi''(\boldsymbol{\xi}, \boldsymbol{\eta})\psi''(\sigma, f) + \Psi^a(\boldsymbol{\xi}, \boldsymbol{\eta})\psi^a(\sigma, f)]\psi^a(\text{color}), \end{aligned} \quad (36)$$

where $\psi(\sigma, f)$ is spin-flavor wave function, while $\psi(\boldsymbol{\xi}, \boldsymbol{\eta})$ is the coordinate one; the superscripts: symm, a , l , ll refer to symmetric, antisymmetric, and two-dimensional representations of 3-body permutation group; note, that $(\boldsymbol{\xi}, \boldsymbol{\eta})$ belong to (ll) representations.

We shall be interested primarily in the neutron state, and since all terms in (36), except for the first one, contain nonzero angular momenta, hence they will be suppressed at large B as compared to the first one [28]. Therefore we can write the combination $\psi^{\text{symm}}(\sigma, f)$ for the neutron with spin down as

$$\begin{aligned} \psi_n^{\text{symm}}(\sigma, f) = & \frac{\sqrt{2}}{6} \{ 2u_+d_-d_- - d_+u_-d_- - u_-d_+d_- + 2d_-u_+d_- - \\ & - d_-d_+u_- - d_+d_-u_- - d_-u_-d_+ - u_-d_-d_+ + 2d_-d_-u_+ \}. \end{aligned} \quad (37)$$

In (37) u_{\pm}, d_{\pm} denote individual quark spin-flavor functions with spin up or down. $\psi_n^{\text{symm}}(\sigma, f)$ is normalized to unity.

The above classification is simple in absence of MF and equal quark masses, since in this case both H_0 (21) and $V_{\text{conf}}^{(\gamma)}$ (32) are symmetric. For nonzero \mathbf{B} three symmetry violations occur: 1) \mathbf{B} violates $O(3)(SU(2))$ symmetry and spin mixing may occur between $J = \frac{1}{2}$ and $J = \frac{3}{2}$ states, 2) \mathbf{B} violates isospin symmetry implying mixing of $I = \frac{1}{2}$ and $\frac{3}{2}$ states, 3) both H_0 and $V_{\text{conf}}^{(\gamma)}$ are not symmetric in quark indices for $B \neq 0$, which implies, that

not all, but only some components of Eq.(37) are dominant ones for strong **B**.

Strictly speaking, when spin and isospin are not good quantum numbers, the Pauli principle applies only to d -quarks in the same state. Both H_0 and $V_{\text{conf}}^{(\gamma)}$ are symmetric with respect to $\boldsymbol{\eta} \leftrightarrow -\boldsymbol{\eta}$, hence the $\phi(\boldsymbol{\eta})$ component in the wave function $\Psi(\xi, \eta) = \phi(\boldsymbol{\eta})\chi(\xi)$ has a symmetry $\phi(\boldsymbol{\eta}) = \phi(-\boldsymbol{\eta})$ and $\psi_n^{\text{symm}}(\sigma, f)$ is symmetric in d, d spin coordinates, but has no definite spin and isospin. The terms $-(d_+d_- + d_-d_+)u_-$ and $d_-d_-u_+$ in (37) meet these conditions. As will be seen, when B is switched on, the neutron state gets splitted into three states (in order of growing energy): $(d_-d_-u_+)$, $(d_-d_+u_-)$, $(d_+d_-u_-)$.

Actually only for two combination $(d_-d_-u_+)$ and $(d_+d_+u_-)$, our equations with $\omega_1 = \omega_2 = \omega$ are valid, and the most general case with arbitrary masses and charges will be considered in the subsequent paper. In the present paper we consider the state $(d_-d_-u_+)$ at large MF $eB \geq \sigma$, where it is dominant for the neutron, and in addition all other states at small MF, where pseudomomentum factorization does not hold but MF can be considered as perturbation.

4 Mass spectrum in MF

The solution of Eq. (33) for the neutral 3q system in MF with confinement, given by Eq.(32) reduces to the solution of four independent oscillator equations. For the lowest $(d_-d_-u_+)$ state this yields

$$\begin{aligned} \frac{M_0(\omega_i, \gamma)}{\sqrt{\sigma}} &= \Omega_{\xi\perp} + \Omega_{\eta\perp} + \frac{1}{2}(\Omega_{\xi\parallel} + \Omega_{\eta\parallel}) + \frac{3\sqrt{\sigma}\gamma}{2} + \\ &+ \frac{m_d^2 + \omega^2 - \frac{\epsilon}{2}B}{\omega\sqrt{\sigma}} + \frac{m_u^2 + \omega_3^2 - eB}{2\omega_3\sqrt{\sigma}}, \end{aligned} \quad (38)$$

where the following notations are used,

$$\Omega_{\xi\perp} = \left[\left(\frac{eB}{4\sigma} \right)^2 \frac{a_+^2}{a^2 a_3^2} + \frac{a_3^2 + 2a^2}{\beta a a_+ d_3} \right]^{1/2}, \quad (39)$$

$$\Omega_{\xi\parallel} = \sqrt{\frac{a_3^2 + 2a^2}{\beta a a_+ a_3}}, \quad (40)$$

$$\Omega_{\eta_{\perp}} = \sqrt{\left(\frac{eB}{4\sigma}\right)^2 \frac{1}{a^2} + \frac{1}{\beta a}}, \quad (41)$$

$$\Omega_{\eta_{\parallel}} = \frac{1}{\sqrt{\beta a}}. \quad (42)$$

Here $\omega = a\sqrt{\sigma}$, $\omega_3 = a_3\sqrt{\sigma}$, $\gamma = \beta/\sqrt{\sigma}$, $a_+ = 2a + a_3$. The resulting parameters a, a_3, β are to be found from the conditions (35), which are written explicitly in the Appendix 1. Directly from (38) it follows that at $eB \rightarrow \infty$ $\bar{M}_0 = M_0(\omega_i^{(0)}, \gamma^{(0)})$ tends to a finite limit. As for the parameters a, a_3 and β , they vary in the limits $1 \geq a, a_3, \beta \gtrsim 0.5$, when eB grows from 0 to infinity. The mass $\bar{M}_0(eB = 0)$ for $m_q = 0$ is equal to $\bar{M}_0 = 6\sqrt{\sigma}$. According to [10] self-energy contribution also depends on MF. For $3q$ system one has

$$\Delta_{SE} = -2\frac{3\sqrt{\sigma}}{4\pi a} \left[1 + \eta(\lambda\sqrt{eB + m_1^2}) \right] - \frac{3\sqrt{\sigma}}{4\pi a_3} \left[1 + \eta(\lambda\sqrt{2eB + m_3^2}) \right], \quad (43)$$

where

$$\eta(t) = t \int_0^{\infty} z^2 K_1(tz) e^{-z} dz. \quad (44)$$

Note, that Δ_{SE} cancels a large part of the meson mass M_0 , which might cast a doubt on the use of Δ_{SE} as a correction. However, this approach was successfully used for the calculation of many meson and baryon masses and Regge trajectories, for baryons see e.g [19, 20], for mesons [31].

In Fig.1 we show the quantity $M_0 + \Delta_{SE}$ as a function of eB . One can see a rapid fall within the interval $0 < eB < 1 \text{ GeV}^2$. Consider now the color Coulomb contribution, i.e., the term $\langle V_{\text{Coul}} \rangle$ with V_{Coul} , given by (24).

The eigenfunctions of $H_0 + V_{\text{conf}}^{(\gamma)}$ can be written in the form

$$\Psi(\boldsymbol{\xi}, \boldsymbol{\eta}) = \psi_1(\xi_{\perp})\psi_2(\xi_{\parallel})\varphi_1(\eta_{\perp})\varphi_2(\eta_{\parallel}), \quad (45)$$

where

$$\begin{aligned} \psi_1(\xi_{\perp}) &= \frac{1}{\sqrt{\pi r_{\xi_{\perp}}^2}} \exp\left(-\frac{\xi_{\perp}^2}{2r_{\xi_{\perp}}^2}\right), & \psi_2(\xi_{\parallel}) &= \frac{1}{(\pi r_{\xi_{\parallel}}^2)^{1/4}} \exp\left(-\frac{\xi_{\parallel}^2}{2r_{\xi_{\parallel}}^2}\right), \\ \varphi_1(\eta_{\perp}) &= \frac{1}{\sqrt{\pi r_{\eta_{\perp}}^2}} \exp\left(-\frac{\eta_{\perp}^2}{2r_{\eta_{\perp}}^2}\right), & \varphi_2(\eta_{\parallel}) &= \frac{1}{(\pi r_{\eta_{\parallel}}^2)^{1/4}} \exp\left(-\frac{\eta_{\parallel}^2}{2r_{\eta_{\parallel}}^2}\right), \end{aligned} \quad (46)$$

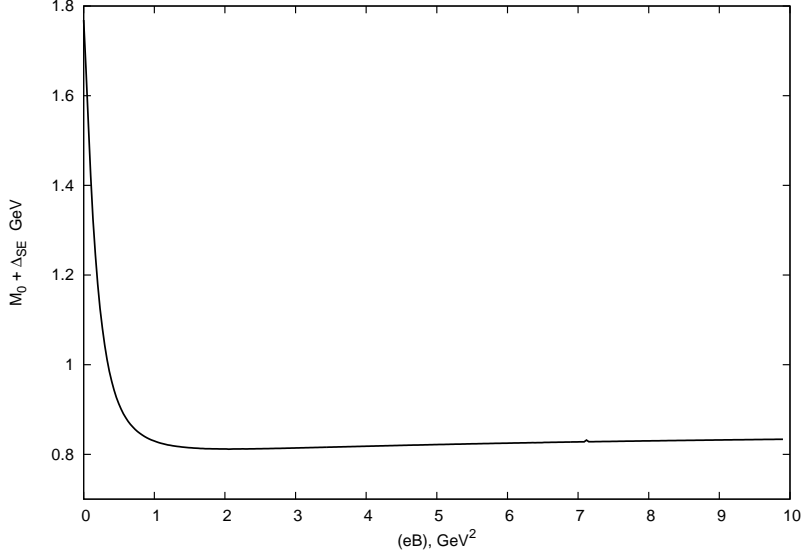


Figure 1: The dynamical baryon mass (without gluon exchange and hf interaction) in GeV as a function of eB .

where

$$\begin{aligned} r_{\xi_{\perp}}^{-2} &= \omega \Omega_{\xi_{\perp}} \cdot \sqrt{\sigma}, & r_{\xi_{\parallel}}^{-2} &= \omega \Omega_{\xi_{\parallel}} \sqrt{\sigma}, \\ r_{\eta_{\perp}}^{-2} &= \omega \Omega_{\eta_{\perp}} \cdot \sqrt{\sigma}, & r_{\eta_{\parallel}}^{-2} &= \omega \Omega_{\eta_{\parallel}} \sqrt{\sigma}. \end{aligned} \quad (47)$$

Momentum space color Coulomb potential with the account of gluon and quark loop effects reads [11]

$$V_{\text{Coul}}(q) = - \frac{16\pi\alpha_s^{(0)}}{3 \left[q^2 \left(1 + \frac{\alpha_s^{(0)}}{4\pi} \frac{11}{3} N_c \ln \left(\frac{q^2 + M_B^2}{\mu_0^2} \right) \right) + \frac{\alpha_s^{(0)} n_f |eB|}{\pi} e^{-\frac{q_{\perp}^2}{2|eB|}} T \left(\frac{q_z^2}{4\sigma} \right) \right]}, \quad (48)$$

where

$$T(z) = \frac{\ln(\sqrt{z+1} + \sqrt{z})}{\sqrt{z(z+1)}} + 1. \quad (49)$$

Inclusion of quark-antiquark loops allows to avoid an unrestricted diminishing of the mass at $eB \rightarrow \infty$. In this way the “fall to the center” in hydrogen atom is prevented [5]. The collapse becomes a real danger only in the $N_c \rightarrow \infty$ limit.

Taking the average of the interquark OGE interaction (24) over the wave function (45) and keeping in mind the relation (3) between \mathbf{z}_i and the Jacobi coordinates, one obtains

$$\Delta M_{\text{Coul}}(\rho_{\perp}(ij), \rho_z(ij)) = \int \frac{d^2 q_{\perp} dq_z}{(2\pi)^3} V(q) e^{-\frac{q_{\perp}^2 \rho_{\perp}^2(s)}{4} - \frac{q_{\parallel}^2 \rho_{\parallel}^2(s)}{4}}. \quad (50)$$

Here

$$\rho_{\perp}^2(12) = \frac{1}{\sqrt{\left(\frac{eB}{4}\right)^2 + \frac{a\sigma^2}{\beta}}}, \quad \rho_{\parallel}^2(12) = \frac{1}{\sigma} \sqrt{\frac{\beta}{a}}; \quad (51)$$

$$\rho_{\perp}^2(13) = \rho_{\perp}^2(23) = \frac{1}{\sqrt{\left(\frac{eB}{2}\right)^2 + 4\sigma^2 \frac{aa_3}{\beta a_+^3} (a_3^2 + 2a^2)}} + \left[\left(\frac{eB}{2}\right)^2 + \frac{4\sigma^2 a}{\beta} \right]^{-1/2}, \quad (52)$$

$$\rho_{\parallel}^2(13) = \frac{1}{2\sigma} \left[\frac{a_+^3 \beta}{a_3 a (a_3^2 + 2a^2)} \right]^{1/2} + \frac{1}{2\sigma} \sqrt{\frac{\beta}{a}}, \quad (53)$$

and $\rho_{\perp}^2(13) = \rho_{\perp}^2(23)$, $\rho_{\parallel}^2(13) = \rho_{\parallel}^2(23)$. Comparing Eq.(50) for $\langle V_{\text{Coul}} \rangle$ with the corresponding expression in case of the $(q\bar{q})$ system in [10], one can see the same structure of the integral (41) in [10] and our Eq. (50), and similar values of parameters ρ_{\perp} and ρ_{\parallel} , which in our case for $eB \rightarrow \infty$ behave as $\frac{2}{\sqrt{eB}}$ and $\frac{1}{\sqrt{\sigma}}$ respectively for $s = 12$, and $\frac{2}{\sqrt{eB}}$ and $\sqrt{\frac{2}{\sigma}}$ for $s = 13, 23$.

This should be compared to the $(q\bar{q})$ parameters $r_{\perp}(eB \rightarrow \infty) = 0$; $r_{\parallel}(eB \rightarrow \infty) = \sqrt{\frac{2}{\sigma}}$. If one represents the color Coulomb correction for a meson as $\Delta M_{\text{Coul}}^{\text{mes}}(r_{\perp}^2, r_{\parallel}^2)$, then for a baryon one can write according to (50)

$$\Delta M_{\text{Coul}}^{\text{bar}} = \frac{1}{2} \Delta M_{\text{Coul}}^{\text{mes}}(\rho_{\perp}^2(12), \rho_{\parallel}^2(12)) + \Delta M_{\text{Coul}}^{\text{mes}}(\rho_{\perp}^2(13), \rho_{\parallel}^2(13)). \quad (54)$$

Now, if one takes the standard Coulomb interaction (i.e. $V(q)$ in (48) without quark loops), we encounter the problem of boundless decrease of the neutron mass at $B \rightarrow \infty$. This phenomenon can be called the ‘‘magnetic collapse of QCD’’, which holds at least in large N_c limit when quark loop contribution becomes negligible. The situation is similar to the hydrogen atom case, where the binding energy diverges as $(-\ln^2 eB)$ [5]. For mesons, as it was shown in [9, 10], $\Delta M_{\text{Coul}}^{\text{mes}}$ diverges as $-\sqrt{\sigma} \ln \ln \frac{eB}{\sigma}$ in the limit $eB \gg \sigma$. In all three

cases - the hydrogen atom, mesons and baryons, the situation is cured by the screening effect produced by the loop contribution in MF. Retaining in (48) the quark loop contribution, one arrives at the nontrivial conclusion that the ground state energy is frozen and the “fall to the center” phenomenon is eliminated [11]. The resulting color Coulomb correction with account of screening effect from (48) is shown on Fig.2.

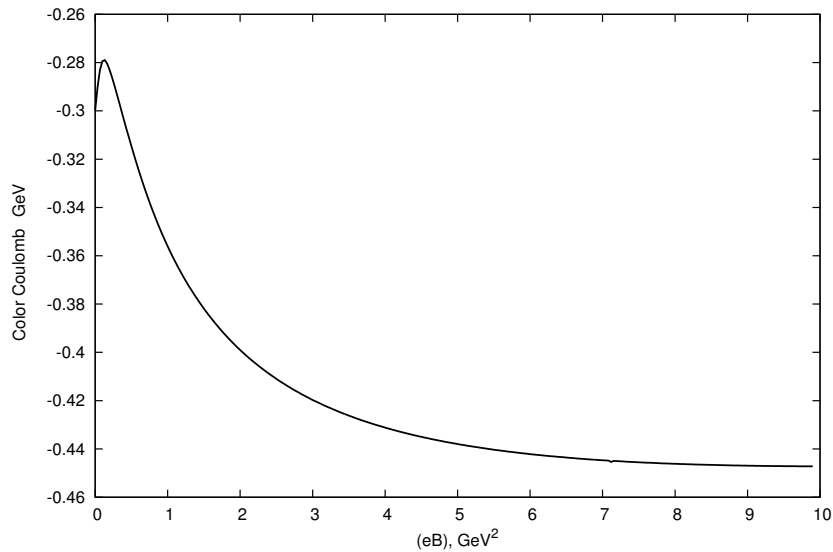


Figure 2: The color Coulomb potential contribution in GeV as a function of eB . One can see a saturation at $eB > 4$ GeV² due to quark loop contribution in the gluon exchange.

5 Spin splittings in MF

Since MF violates both spin and isospin symmetries, one must diagonalize the spin-dependent terms of the Hamiltonian (22) in order to find its solutions. The spin-dependent piece is

$$\begin{aligned}
 h_\sigma &= \Delta_{ss}^{\text{pert}} + V_\sigma = \Delta_{ss}^{\text{pert}} - \sum_{i=1}^3 \frac{e_i \sigma_z^{(i)} B}{2\omega_i} \equiv \\
 &\equiv d\sigma_3(\sigma_1 + \sigma_2) + b\sigma_1\sigma_2 - c_3\sigma_{3z} + c(\sigma_{1z} + \sigma_{2z}), \quad (55)
 \end{aligned}$$

where

$$d = \frac{4\alpha_s}{9\omega\omega_3} \langle \delta(\mathbf{r}_{31}) \rangle, \quad b = \frac{4\alpha_s}{9\omega^2} \langle \delta(\mathbf{r}_{12}) \rangle, \quad (56)$$

$$c = \frac{eB}{4\omega}, \quad c_3 = \frac{eB}{2\omega_3}. \quad (57)$$

These expressions are valid for the state $| - - + \rangle$. In the more general case coefficients in front of σ_{1z} and σ_{2z} as well as in front of $\sigma_3\sigma_1$ and $\sigma_3\sigma_2$ should differ.

The mixing between the $S = 1/2$ and $S = 3/2$ states is due to the term $d\sigma_3(\sigma_1 + \sigma_2)$. Writing the 3q spin-flavor wave function for total spin projection $(-\frac{1}{2})$ in a simplified form (to be symmetrized in (123)), one has

$$\Psi_{-\frac{1}{2}} = \alpha(- - +) + \frac{\beta}{\sqrt{2}}[(+ - -) + (- + -)], \quad \alpha^2 + \beta^2 = 1. \quad (58)$$

Note, that the spin-independent part of the total Hamiltonian has a diagonal form with respect to spin variables, but diagonal elements are spin-dependent, since the quantities ω_i for the states with different spin projections are defined by a different minimization conditions. So, for the state $(- - +)$ all ω_i and resulting mass \bar{M}_0 tend to the finite limit at large eB , while for the state $\frac{1}{\sqrt{2}}[(+ - -) + (- + -)]$ we have one bounded and two growing ω_i at large eB . The resulting mass for this state grows unboundedly with increase of MF.

At zero MF the initial values of α and β are: for the neutron $\alpha_n = \sqrt{\frac{2}{3}}$, $\beta_n = -\frac{1}{\sqrt{3}}$, and for the Δ -isobar $\alpha_\Delta = \frac{1}{\sqrt{3}}$, $\beta_\Delta = \sqrt{\frac{2}{3}}$. Consequently one finds the ‘‘trajectory’’ of the neutron mass going down with eB and that of the Δ mass going up. We shall denote these combinations n_B and Δ_B , their wave functions are described by (58) with the corresponding α and β . In the limit $eB \rightarrow \infty$ we have $\alpha_n = 1$, $\beta_n = 0$ and $\alpha_\Delta = 0$, $\beta_\Delta = 1$, which corresponds to the disappearance of mixing. In the general case for a finite MF the ratio of coefficients β/α for neutron (or α/β for Δ) is suppressed. Hence $| - - + \rangle$ is a good approximation for lowest mass state, which gives the dominant contribution for $eB \geq \sigma$.

The trajectory n_B without the hf interaction tends to a positive constant at $eB \rightarrow \infty$. The inclusion of the hf interaction at large MF can make the neutron mass negative, since $\langle V_{\text{hf}} \rangle \propto eB$. However, it was proved that MF cannot make the mass vanish due to spin-dependent forces [18], therefore considering the hf interaction as a perturbation, one should use the smearing

factor with the smearing radius of $(0.1 \div 0.2)$ fm [13, 29, 30]. As will be seen below, this procedure still does not prevent vanishing of $M_n(eB)$ at large $eB \sim 1$ GeV², which implies the importance of higher order hf interaction terms, which must ensure the positivity of $M_n(eB)$ at all values of eB .

The $3q$ Green's function generated by the $3q$ current $J_{\mu_1\mu_2\mu_3}$ is proportional to

$$G \sim \langle J|n_B \rangle \exp(-iM(n_B)t) \langle n_B|J \rangle + \langle J|\Delta_B \rangle \exp(-iM(\Delta_B)t) \langle \Delta_B|J \rangle \quad (59)$$

and therefore will display the pattern of mass oscillation depending on MF. This is similar to the neutrino mass oscillations, but strongly differs in scale.

6 Baryon mass spectrum at varying MF

In what follows we shall be interested primarily in the trajectory n_B and shall use for $eB \geq \sigma$ the diagonal element of the total Hamiltonian describing the $|- - + \rangle$ component. The mass (energy) eigenvalue is

$$M_n = E + (b - 2d), \quad (60)$$

where E is the solution of (33), written with account of the self-energy Δ_{SE} and the Coulomb $\langle V_{\text{Coul}} \rangle$ corrections:

$$E = M_0 + \Delta_{SE} + \langle V_{\text{Coul}} \rangle. \quad (61)$$

The parameters b and d are defined in (56), (57), the explicit expressions for $\langle \delta(\mathbf{r}_{ij}) \rangle$ are given in the Appendix 2.

The quantities V_{Coul} and Δ_{SE} are evaluated making use of the variational averaging procedure, hence one should find the stationary value of M_0 from the conditions (35), where M_0 is given in (38).

As a result one obtains $\bar{M}_0 = M_0(\omega^{(0)}, \omega_3^{(0)}, \gamma^{(0)})$, with parameters taken at stationary points. In this way $\bar{M}_0(B)$ is obtained. The starting point is $eB = 0$, where one has from Appendix 3 (expression (60) is not a good approximation for zero MF)

$$M_{\pm} = E + b - d \pm 3d, \quad (62)$$

so the $n - \Delta$ mass difference is $6d \cong 0.15\alpha_s\sqrt{\sigma} \approx 20$ MeV for $\alpha_s = 0.35$ and $6d \approx 100$ MeV for $\alpha_s = 1.72$.

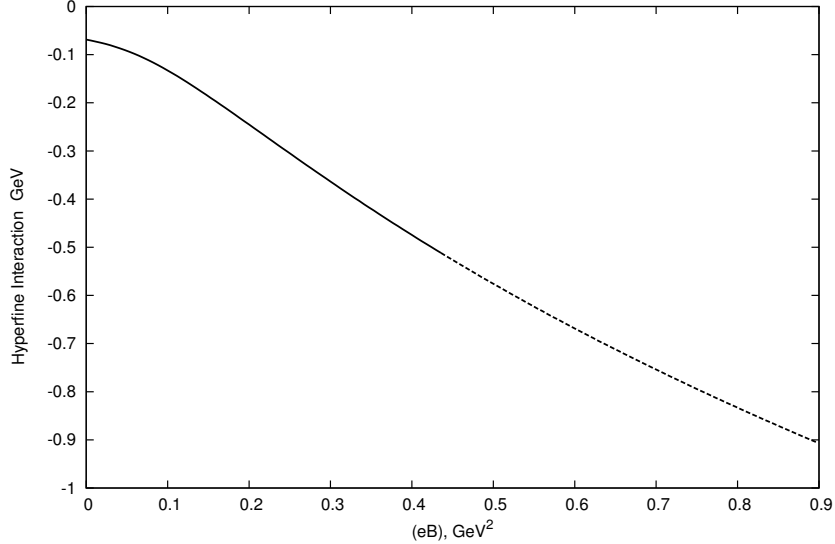


Figure 3: The hyperfine diagonal contribution $\langle V_{hf} \rangle = \tilde{b} - 2\tilde{d}$ from Eq.(64) to the neutron mass in GeV as a function of eB .

Thus we see, that $\Delta_{ss}^{\text{pert}}$ by itself does not ensure the experimental splitting between n and Δ close to 300 MeV. As it is well known [22], this difference can be explained adding the OPE interaction, having the same $\sigma_i \sigma_j$ structure. Therefore one has to include the OPE quark-antiquark interaction

$$V_{\text{ope}}^{(ij)}(\mathbf{k}) = 4\pi g_{qq\pi}^2 \boldsymbol{\tau}(i) \boldsymbol{\tau}(j) \frac{\Gamma_i \Gamma_j}{\mathbf{k}^2 + m_\pi^2} \left(\frac{\Lambda^2}{\Lambda^2 + \mathbf{k}^2} \right)^2, \quad (63)$$

where $\Gamma_i = \frac{\boldsymbol{\sigma}(i)\mathbf{k}}{\omega_i + m_i}$, $\omega = \sqrt{\mathbf{k}^2 + m_i^2}$. Comparing V_{ope} (63) with Δ_{ss} (56), one can see that both have the similar structure in the p -space, since for vanishing masses $m_u = m_d = m_\pi = 0$ one has in (63) the structure $\frac{(\boldsymbol{\sigma}(i)\mathbf{k})(\boldsymbol{\sigma}(j)\mathbf{k})}{\omega_i \omega_j k^2} \rightarrow \frac{\boldsymbol{\sigma}(i)\boldsymbol{\sigma}(j)}{\omega_i \omega_j}$. Numerically, as shown in [22] for $\sigma = 0.12 \text{ GeV}^2$ the contribution of $\bar{V}_{ss} = \sum_{i>j} (V_{hf}^{(ij)} + V_{\text{ope}}^{(ij)})$ to n and Δ masses are (-471 MeV) and (-79 MeV) respectively. Therefore after summing $\Delta_{ss}^{\text{pert}}$, Eq.(55) and V_{ope} , Eq.(63), we introduce the new hf interaction

$$V_{hf} = \Delta_{ss}^{\text{pert}} + V_{\text{ope}} \simeq \tilde{d}\sigma_3(\sigma_1 + \sigma_2) + \tilde{b}\sigma_1\sigma_2, \quad (64)$$

where the form (56) with α_s replaced by $\alpha_{hf} = \alpha_s + \alpha_{\text{ope}}$, and α_{ope} takes into account the pion charge structure of Eq.(67), see Appendix 3 for details.

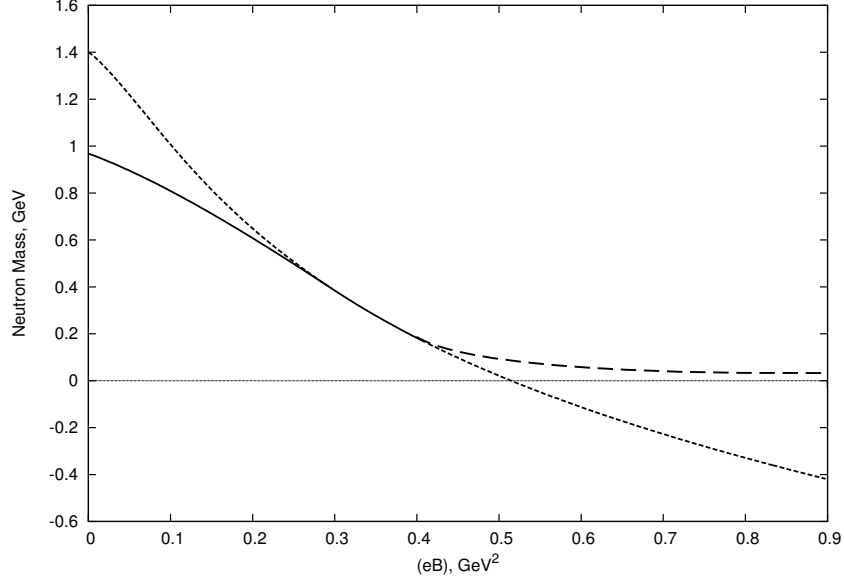


Figure 4: The neutron mass with hf correction included vs eB , the solid line: refers to the region where approximation made are reliable. The dotted line refers to the state $|--+\rangle$ with hf as a perturbation. Dashed line shows a possible form of the behaviour, satisfying the stabilization theorem

The difficulty we encounter here is that in order to get a correct answer it is necessary to take into account the mixing of different spin states at $eB \ll \sigma$ (see (58)). While keeping only the state $|--+\rangle$ the neutron mass at $eB \ll \sigma$ exceeds the experimental value.

Consider now the OPE interaction at growing eB . We have to split the OPE interaction into the contributions from π^+ , π^- and π^0 mesons.

$$V_{\text{ope}}^{ij} = \frac{4\pi g^2}{\omega_i \omega_j} \left[\frac{(\boldsymbol{\sigma}_i \cdot \mathbf{k})(\boldsymbol{\sigma}_j \cdot \mathbf{k})}{k^2 + m_{\pi^+}^2} 2\tau_+^i \tau_-^j + \frac{(\boldsymbol{\sigma}_i \cdot \mathbf{k})(\boldsymbol{\sigma}_j \cdot \mathbf{k})}{k^2 + m_{\pi^-}^2} 2\tau_-^i \tau_+^j + \frac{(\boldsymbol{\sigma}_i \cdot \mathbf{k})(\boldsymbol{\sigma}_j \cdot \mathbf{k})}{k^2 + m_{\pi^0}^2} \tau_3^i \tau_3^j \right] \left(\frac{\Lambda^2}{k^2 + \Lambda^2} \right)^2. \quad (65)$$

As it was shown analytically in [12] and on the lattice [32], the π^\pm masses grow with MF as $\sim \sqrt{eB}$. Therefore the first two terms in (65) are suppressed at large eB . On the other hand, the mass of π_0 becomes somewhat smaller [12] and its contribution into V_{ope} important in the whole interval of MF. Hence only the last term in (67) survives in the large eB limit. That's why

$\alpha_{\text{ope}}(eB \gg \sigma) \simeq \frac{1}{3}\alpha_{\text{ope}}(B = 0)$. Being averaged over the $|ddu\rangle$ isospin state and over the wave function (45), the OPE and spin-spin interaction operators have the same structure with the only qualitative difference concerning the smearing procedure of the δ -function - the gaussian one for the spin-spin [10] and the Yukawa form-factor for OPE. This difference is of a minor importance for the dependence of the interaction on MF. Therefore both corrections can be treated in a uniform way by the introduction of the effective hyperfine interaction constant α_{hf} . Here one must distinguish two regions 1) $eB \leq \sigma$, 2) $eB \geq \sigma$. In the first one must keep all terms of the wave function as in (58), and calculate the ground state of h_σ (55), as shown in Appendix 3. Here α_{hf} is chosen to reproduce the $\Delta - n$ splitting of 300 MeV. In the second region one keeps only the dominant $|--+\rangle$ state, and uses Eq.(60) to calculate $M_n(B)$, the exact procedure and numerical values are given in Appendix 3. The result is shown in Fig.3. The main general conclusion is that the spin-spin interaction is extremely sensitive to MF. Due to the Fermi-Breit δ -type interaction the mass tends to cross the $M = 0$ value at $eB \sim 2\sigma$, while the general statement (see [18]) forbids this happen. This means that for δ -type interactions the perturbation theory fails to lead to physically correct results in the limit of strong MF. One has to develop an alternative approach to treat hyperfine interaction in MF.

7 Discussion of the results

At this point one must look more closely at the problem of the hyperfine interaction in baryons. It was understood rather early (see e.g. the discussion in [34, 33]), that the standard hf interaction is too weak for a reasonable α_s to explain the 300 MeV splitting between the masses of Δ and nucleon. This is contrast to the meson case, when the $q\bar{q}$ hf interaction yields $\simeq 200$ MeV splitting of ρ and π masses, and in addition the Nambu-Goldstone mechanism shifts the pion mass to its proper place. In baryon with $\alpha_s(m_N) \sim 0.5$ one obtains the splitting around 35 MeV instead of 300 MeV. To save the situation in [34] the authors have used the smeared form of the hf potential to all orders, which strongly enhanced the hf contribution: as shown in [33] for the smearing parameter $\lambda = 1.5$ GeV the hf splitting grows approximately 10 times, when taken to all orders of the V_{hf} , derived in the first order of α_s .

Another approach was used in [35], where the instanton interaction was parametrised to increase the hf contribution.

Instead we have used a more physical mechanism, which should anyhow be present in the $3q$ system: the pion exchange. We have shown based on earlier papers [22], that the pion exchange strongly increases the resulting gap in masses and can ensure the physical splitting (in absence of MF) for reasonable values of pion coupling with quarks.

However for growing MF one encounters several difficulties. First of all, the pseudomomentum factorization (4), which is the basis of our present approach, requires equality of masses and energies $m_1 = m_2$, $\omega_1 = \omega_2$, which is true only for the state $|ddu\rangle \otimes |--+\rangle$. Now this state is the main component of the ground state for $eB \gg \sigma$, and therefore one obtains a reliable result for the neutron mass in this region before the inclusion of the hf interaction. However, including the hf interaction with the pion exchange at strong MF one immediately obtains a huge shift down of the neutron mass, making it negative around $eB \sim 0.5 \text{ GeV}^2$.

This happens both with or without the pion exchange term, provided the starting $\Delta - n$ splitting is around 300 MeV, and the problem is that the resulting hf shift at the perturbative level is huge, and violates the theorem of [18], stating, that MF cannot make the hadron mass to become negative. As shown in [18], when mass tends to zero in MF, the Dirac eigenvalues of all quarks can condense near the zero point, similarly to the case of the chiral symmetry breaking phenomenon, and may ensure the mass to be nonzero, however small. We illustrate this behavior in Fig.4 by a dashed line, which gives the idea of true trajectory, satisfying the stabilization theorem of [18].

At small MF we have another difficulty - inapplicability of the pseudomomentum factorization (4), when all components of the wave function are taken into account, and to proceed, we have used the limit of small MF and calculated the neutron mass up to the order $(\frac{eB}{\sigma})^2$, (polarizability region), using all components of the wave function. This result, valid for $eB < 0.15 \text{ GeV}^2$, is shown in Fig.4 by a piece of a solid line below the dotted line, the latter depicts the mass of the state $|--+\rangle$, continued to the region of small eB , where it is not reliable. The regime of the strong MF ($eB > \sigma$), is depicted by a dotted line in Fig.4. Thus the pseudomomentum factorization method with the $|--+\rangle$ component provides the results, shown in Fig.4 by a dotted line. At larger eB one assumes the saturating behavior, shown by a dashed line, while the dotted line describes the behavior predicted by the first order perturbation theory. Thus the solid line in Fig.4 shows the results obtained within the reliable approximations.

8 Conclusions

In our treatment of the relativistic $3q$ system embedded in MF we relied on pseudomomentum factorization of the wave function and the relativistic Hamiltonian technique. To our knowledge this is the first investigation of the three-body system with relativistic interaction in the external MF. The focus was on the dependence of the neutron mass on MF. This problem was solved analytically with confinement, color Coulomb and spin-spin interactions taken into account. From the physical arguments it is clear that MF starts to produce drastic variation of the neutron mass as soon as its strength approaches the string tension, $eB \sim \sigma \sim 10^{19} \text{ G} \sim 0.2 \text{ GeV}^2$. Our calculations confirm this conclusion. In strong MF the ground state of ddu system has the spin structure $| - - + \rangle$. An intriguing question is whether the mass of this state goes to zero in the limit $eB \rightarrow \infty$. This "fall to the center" phenomenon might happen for two reasons. The first one is the color Coulomb interaction. This kind of collapse is avoided due to quark-antiquark loops in the same way, as it happens in quark-antiquark system, or in the hydrogen atom due to e^+e^- loops. The second potential source of collapse is the spin-spin interaction which is proportional to the delta-function and gives a contribution growing linearly with eB . How to treat this interaction beyond the perturbation theory is an old and still unresolved problem. The standard way to overcome this difficulty is to smear a delta-function around the origin with some characteristic range. For the quark system this range is given by the correlation length of the gluon field equal to 0.1 – 0.2 fm. However, even with smearing the neutron mass can become zero at a finite value of eB and, as it shown in [18] this cannot happen for any value of eB in the exact treatment, and the mass vanishing is the result of unlawful use of perturbation theory. Instead, the condensation of the quasi-zero Dirac eigenmodes may prevent this type of collapse.

In future study this line of research can be continued in several directions. Our method allow to consider the phase transition between neutron and quark matter in MF. This problem is of outmost importance for the neutron stars physics.

9 Acknowledgements

The authors are thankful to M.I. Vysotsky, S.I. Godunov and A.E. Shabad for remarks and discussions.

Appendix 1 Solution of the system of equations (35)

In terms of a, a_3, β the Eqs. (35) can be written as

$$\frac{\partial}{\partial a} \left(\Omega_{\xi\perp} + \Omega_{\eta\perp} + \frac{1}{2}\Omega_{\xi\parallel} + \frac{1}{2}\Omega_{\eta\parallel} \right) - \frac{m_d^2 - \frac{e}{2}B}{a^2\sigma} + 1 = 0, \quad (1.1)$$

$$\frac{\partial}{\partial a_3} \left(\Omega_{\xi\perp} + \Omega_{\eta\perp} + \frac{1}{2}\Omega_{\xi\parallel} + \frac{1}{2}\Omega_{\eta\parallel} \right) - \frac{m_u^2 - eB}{2a_3^2\sigma} + \frac{1}{2} = 0, \quad (1.2)$$

$$\frac{\partial}{\partial \beta} \left(\Omega_{\xi\perp} + \Omega_{\eta\perp} + \frac{1}{2}\Omega_{\xi\parallel} + \frac{1}{2}\Omega_{\eta\parallel} \right) + \frac{3}{2} = 0. \quad (1.3)$$

Using (39)-(42), one can calculate all terms in (1.1)-(1.3). We shall explicitly write down the results in two opposite limits: $eB = 0$ and $eB \rightarrow \infty$.

a) $eB = 0$. In this case $a_3 = a$ and, neglecting quark masses m_u, m_d , one has

$$\frac{M_0}{\sqrt{\sigma}} = \frac{3}{\sqrt{\beta a}} + \frac{3}{2}(a + \beta). \quad (1.4)$$

Eq. (1.1) yields $a = \beta^{-1/3}$. From (1.3) one has $\beta = a^{-1/3}$, which results in $a(eB = 0) = \beta(eB = 0) = 1$.

b) $eB \rightarrow \infty$. In this case (1.1)-(1.3) yield correspondingly

$$4a^{3/2}\beta^{1/2} = 1 + \frac{\sqrt{x}(x^2 + 4x - 2)}{(2+x)^{3/2}(2+x^2)^{1/2}}, \quad (1.5)$$

$$a^{3/2}\beta^{1/2} = \frac{2 + 2x - x^2}{(2+x)^{3/2}x^{3/2}(2+x^2)^{1/2}}, \quad (1.6)$$

$$6a^{1/2}\beta^{3/2} = 1 + \sqrt{\frac{x^2 + 2}{x(x+2)}}, \quad (1.7)$$

where $x \equiv \frac{a_3}{a}$. Numerical solution of (1.5)-(1.7) yields $x = 1$, $\beta/a = 1$, and finally one obtains

$$a(eB \rightarrow \infty) = a_3(eB \rightarrow \infty) = \beta(eB \rightarrow \infty) = \frac{1}{\sqrt{3}}. \quad (1.8)$$

Appendix 2 Hyperfine matrix elements

To calculate $\langle \delta(\mathbf{r}_{13}) \rangle$ one can use wave functions (45)-(47) and the relations

$$\mathbf{r}_{13} \equiv \mathbf{z}_1 - \mathbf{z}_3 = \frac{1}{2} \left(\sqrt{\frac{2\omega_+}{\omega_3}} \boldsymbol{\xi} - \sqrt{2} \boldsymbol{\eta} \right), \quad \mathbf{r}_{12} = \sqrt{2} \boldsymbol{\eta}, \quad (2.1)$$

which yields

$$\langle \delta(\mathbf{r}_{13}) \rangle = 2^{3/2} \int \psi_1^2(\boldsymbol{\xi}_\perp) \psi_2^2(\xi_\parallel) \varphi_1^2 \left(\sqrt{\frac{\omega_+}{\omega_3}} \boldsymbol{\xi}_\perp \right) \varphi_2^2 \left(\sqrt{\frac{\omega_+}{\omega_3}} \xi_\parallel \right) d^3 \xi. \quad (2.2)$$

Inserting in (2.2) the explicit expressions (46), (47), one has

$$\langle \delta(\mathbf{r}_{13}) \rangle = \left(\frac{2a\sigma}{\pi} \right)^{3/2} \frac{\Omega_{\xi_\perp} \Omega_{\eta_\perp}}{\Omega_{\xi_\perp} + \frac{\omega_\pm}{\omega_3} \Omega_{\eta_\perp}} \left[\frac{\Omega_{\xi_\parallel} \Omega_{\eta_\parallel}}{\Omega_{\xi_\parallel} + \frac{\omega_\pm}{\omega_3} \Omega_{\eta_\parallel}} \right]^{1/2}, \quad (2.3)$$

$$\langle \delta(\mathbf{r}_{12}) \rangle = \left(\frac{a\sigma}{2\pi} \right)^{3/2} \Omega_{\eta_\perp} \Omega_{\eta_\parallel}^{1/2}. \quad (2.4)$$

Now we replace $\delta(\mathbf{r})$, for which the perturbation theory is unlawful, by a smeared out version

$$\delta^{(3)}(\mathbf{r}) \rightarrow \tilde{\delta}^{(3)}(\mathbf{r}) = \left(\frac{1}{\lambda\sqrt{\pi}} \right)^3 e^{-\mathbf{r}^2/\lambda^2}, \quad \lambda \sim 1 \text{ GeV}^{-1}. \quad (2.5)$$

With this function we obtain

$$\begin{aligned} \langle \tilde{\delta}^{(3)}(\mathbf{r}_{13}) \rangle &= \left(\frac{2a\sigma}{\pi} \right)^{3/2} \left[1 + \frac{2\lambda^2 a_3}{a_+} a\sigma \Omega_{\xi_\perp} \right]^{-1} \left[1 + \frac{2\lambda^2 a_3}{a_+} a\sigma \Omega_{\xi_\parallel} \right]^{-1/2} \times \\ &\Omega_{\xi_\perp} \Omega_{\eta_\perp} \Omega_{\xi_\parallel}^{1/2} \Omega_{\eta_\parallel}^{1/2} \left[\frac{a_+ \Omega_{\eta_\perp}}{a_3} + \frac{\Omega_{\xi_\perp}}{1 + \frac{2\lambda^2 a_3}{a_+} a\sigma \Omega_{\xi_\perp}} \right]^{-1} \left[\frac{a_+ \Omega_{\eta_\parallel}}{a_3} + \frac{\Omega_{\xi_\parallel}}{1 + \frac{2\lambda^2 a_3}{a_+} a\sigma \Omega_{\xi_\parallel}} \right]^{-1/2}, \end{aligned} \quad (2.6)$$

$$\langle \tilde{\delta}^{(3)}(\mathbf{r}_{12}) \rangle = \left(\frac{a\sigma}{\pi} \right)^{3/2} \Omega_{\eta_\perp} \Omega_{\eta_\parallel}^{1/2} \frac{1}{2 + \lambda^2 a\sigma \Omega_{\eta_\perp}} \frac{1}{\sqrt{2 + \lambda^2 a\sigma \Omega_{\eta_\parallel}}}. \quad (2.7)$$

Eqs. (39)-(42) help to express the r.h.s. of (2.6), (2.7) in terms of a_3, a, β .

Appendix 3 Baryon mass in weak MF

Calculation of the mass spectrum of the 3q system in weak MF in our formalism is similar to the calculation of the Zeeman splitting in ordinary quantum mechanics. First of all, one should fix values of $a_0 = a(B = 0)$, $a_{30} = a_3(B = 0)$ and $\gamma_0 = \gamma(B = 0)$ for the zero MF, i.e. we exclude any influence of the MF over the dynamics and spatial wave function. The next step is to treat magnetic moments and hyperfine terms as a perturbation around the $E_0 = E(B = 0)$ from Eq.(61). The third step is to diagonalize the spin-dependent Hamiltonian (55) (with \tilde{d} and \tilde{b} from (64)) with respect to the 3q spin-flavor wave function with total spin projection $(-\frac{1}{2})$

$$h_\sigma = \tilde{d}\sigma_3(\sigma_1 + \sigma_2) + \tilde{b}\sigma_1\sigma_2 - c_3\sigma_{3z} + c(\sigma_{1z} + \sigma_{2z}), \quad (3.1)$$

$$\Psi_{-\frac{1}{2}} = \alpha(- - +) + \frac{\beta}{\sqrt{2}}[(+ - -) + (- + -)], \quad \alpha^2 + \beta^2 = 1. \quad (3.2)$$

After straightforward manipulations one has for n and Δ^0

$$M_\pm = E_0 + \tilde{b} - \tilde{d} - c \pm \sqrt{8\tilde{d}^2 + (c + c_3 + \tilde{d})^2}, \quad (3.3)$$

The final step is to choose an appropriate $\alpha_{hf} = \alpha_s + \alpha_{\text{ope}}$ constant. There are three key points the choice is based on: first of all the hf interaction should provide the proper value of the splitting between the n and Δ^0 at zero MF, this requirement gives us $\alpha_{hf}(B = 0) = 17$. The second point is that in high MF limit $\alpha_{\text{ope}}(eB \gg \sigma) \simeq \frac{1}{3}\alpha_{\text{ope}}(B = 0)$ since only π^0 contribution survives at high eB . The third point is that in the intermediate region near the $eB \sim \sigma$ these two trajectories should have a smooth connection, which provides $\alpha_{hf}(eB \gg \sigma) = 7$. This situation takes place only if $\alpha_s = 2$ and $\alpha_{\text{ope}}(B = 0) = 3\alpha_{\text{ope}}(eB \gg \sigma) = 15$.

References

- [1] D.E. Kharzeev, K. Landsteiner, A. Schmitt, and H.-U. Yee, Lect. Notes Phys. **871**, 1 (2013).
- [2] D.E. Kharzeev, L.D. McLerran and H.J. Warringa, Nucl. Phys. **A803**, 227 (2008); V. Skokov, A. Illarionov and V. Toneev, Int. J. Mod. Phys. **A24**, 5925 (2009).

- [3] A. Y. Potekhin, Phys. Usp. **53**, 1235 (2010); A. K. Harding and Dong Lai, Rept. Prog. Phys. **69**, 2631 (2006).
- [4] R. Gatto and M. Ruggieri, Phys.Rev. D **83**, 034016 (2011); J. O. Andersen and R. Khan, Phys.Rev. D **85**, 065026 (2012); M. D’Elia, S. Mukherjee, F. Sanfilippo, Phys.Rev. D **82**, 051501 (2010); V. Dexheimer, R. Negreiros, S. Schramm, J.Phys.Conf.Ser. **432**, 012005 (2013).
- [5] A. E. Shabad and V. V. Usov, Phys. Rev. **D73**, 125021 (2006); B. Machedet and M. I. Vysotsky, Phys. Rev. **D83**, 025022 (2011); S. I. Godunov, B. Machedet and M. I. Vysotsky, Phys. Rev. **D85**, 044058 (2012).
- [6] A.E. Shabad and V.V. Usov, Phys. Rev. Lett. **98**, 180403 (2007).
- [7] Y. Hidaka and A. Yamamoto, Phys.Rev. D **87**, 094502 (2013).
- [8] V. V. Braguta, P. V. Buividovich, M. N. Chernodub, A. Yu. Kotov, M. I. Polikarpov, Phys. Lett. B **718**, 667 (2012); E. V. Luschevskaya and O. V. Larina, arXiv:1306.2936 [hep-lat].
- [9] M. A. Andreichikov, B. O. Kerbikov, and Yu. A. Simonov, arXiv:1210.0227 [hep-ph].
- [10] M. A. Andreichikov, B. O. Kerbikov, V. D. Orlovsky, and Yu. A. Simonov, Phys. Rev. D **87**, 094029 (2013).
- [11] M. A. Andreichikov, V. D. Orlovsky, and Yu. A. Simonov, Phys. Rev. Lett. **110**, 162002 (2013).
- [12] V. D. Orlovsky and Yu. A. Simonov, JHEP 1309, 136 (2013), arXiv:1306.2232 [hep-ph].
- [13] J. Alford and M. Strickland, Phys.Rev. D **88**, 105017 (2013), arXiv:1309.3003; C. S. Machado et al., Phys. Rev. D **88**, 034009 (2013).
- [14] Yu. A. Simonov, Nucl. Phys. **B307**, 512 (1988); Yu. A. Simonov and J. A. Tjon, Ann. Phys. (N.Y.) **300**, 54 (2002).
- [15] Yu. A. Simonov, Phys. Rev. D **88**, 025028 (2013), arXiv:1303.4952 [hep-ph].

- [16] M. A. Andreichikov, B. O. Kerbikov, Yu. A. Simonov, arXiv:1304.2516 [hep-ph].
- [17] Yu. A. Simonov, arXiv:1308.5553 [hep-ph].
- [18] Yu. A. Simonov, Phys. Rev. D **88**, 053004 (2013)
- [19] Yu. A. Simonov, Phys. Atom. Nucl. **66**, 338 (2003).
- [20] Yu. A. Simonov, Phys. Rev. D **65**, 116004 (2002).
- [21] Yu. A. Simonov, Phys. Atom. Nucl. **74**, 1223 (2011).
- [22] Yu. A. Simonov, J. A. Tjon, J. Weda, Phys.Rev. D **65**, 094013 (2002).
- [23] W. E. Lamb, Phys. Rev. **85**, 259 (1952); L.P. Gor'kov and I.E. Dzyaloshinskii, Soviet Physics JETP, **26**, 449 (1968); J.E. Avron, I.W. Herbst, and B. Simon, Ann.Phys. (NY), **114**, 431 (1978); H. Grotzsch and R.A. Hegstrom, Phys. Rev. **A4**, 59 (1971).
- [24] B. O. Kerbikov and Yu. A. Simonov, Phys. Rev. D**62**, 093016 (2000).
- [25] Yu. A. Simonov, Phys. Lett **B719**, 464 (2012).
- [26] H. Herold, H. Ruder, and G. Wunner, J. of Phys. **B14**, 751 (1981).
- [27] Yu. A. Simonov, Phys. Lett **B515**, 137 (2001).
- [28] A. M. Badalian, Yu. A. Simonov, Sov. J. Nucl. Phys. **3**, 755 (1966); F. Calogero and Yu. A. Simonov, Phys. Rev. **183**, 869 (1969); M. Fabre de la Ripelle, J. Navarro, Ann. Phys. (N.Y.) **123**, 185 (1979).
- [29] B.O. Kerbikov, M.I. Polikarpov, and L.V. Shevchenko, Nucl Phys. **B331**, 19 (1990).
- [30] T. Kawanai and S. Sasaki, Phys. Rev. **D85**, 091503 (2012).
- [31] A.M. Badalian, B.L.G. Bakker, Yu.A. Simonov, Phys. Rev. **D66**, 034026 (2002).
- [32] G.S. Bali, F. Bruckmann, G. Endrödi et al., Phys. Rev. **D86**, 071502 (2012)

- [33] I.M. Narodetskii, Yu.A. Simonov and V.P. Yurov, *Z. Phys.* **C3**, 55, 695 (1992).
- [34] S. Capstick and N. Isgur, *Phys. Rev.* **D34** 2809 (1986).
- [35] U. Loering, K. Kretzschmar, B.C. Metsch et al., *Eur. Phys. J.* **A10**, 309 (2001), arXiv:hep-ph/0103287; B. Metsch, arXiv:hep-ph/9712246; B. Metsch and U. Loering, *PiN Newslett.* **16** 225 (2002), arXiv:hep-ph/0110415.